New Experimental Procedures for *in vivo* L-band and Radio Frequency EPR Spectroscopy/Imaging

Silvia Colacicchi,[b] Marcello Alecci,[a] Giancaterino Gualtieri,[a] Valentina Quaresima,[a] Cinzia Lucia Ursini,[a] Marco Ferrari[a] and Antonello Sotgiu[a]
[a] *Dip. Scienze e Tecnologie Biomediche, Universita' dell' Aquila, Collemaggio, 67100 L'Aquila, Italy*
[b] *Centro di Risonanza Magnetica, Universita' dell' Aquila, Collemaggio, 67100 L'Aquila, Italy*

Electron paramagnetic resonance spectroscopy/imaging experiments are currently being performed on small animals and isolated organs. The exogenous paramagnetic probes commonly used are nitroxide (aminoxyl) free radicals. Nitroxide reduction and clearance were evaluated to understand *in vivo* distribution and metabolism. Pharmacokinetics data were collected with the same nitroxide at three different frequencies in an external rat blood circuit, in a mouse head and in a whole rat body. A 280 MHz spectrometer made it possible to obtain images of a whole rat body after nitroxide intravenous injection. At L-band (1500 MHz), a synchronization technique was used to obtain images of a dynamic phantom utilized to mimic the model of the isolated perfused rat heart. Different experimental procedures are discussed and the problems which affect sensitivity and resolution are evaluated.

Electron paramagnetic resonance imaging (EPRI) is currently being explored for the study of living systems. The endogenous paramagnetic species produced *in vivo* by physiopathological processes have half-lives and concentrations which do not permit their direct detection. Therefore exogenous paramagnetic probes must be employed. The most commonly used probes are nitroxide free radicals, which combine low toxicity with the possibility to determine oxygen concentration. This can be done either through the determination of their line width and/or through the study of their reduction rate. Recently, new paramagnetic probes, such as fusinite and lithium phthalocyanine,[1] have been proposed and tested for the *in vivo* determination of very low oxygen concentrations. In order to improve image resolution a very narrow line width is necessary, and for this reason deuteriated and perdeuteriated nitroxides are used. Table 1 reports different paramagnetic probes that have been tested *in vivo* for EPR spectroscopy and EPRI.

EPR spectroscopy is performed in a wide range of operating frequencies, from radio frequencies (RF) to far-infrared.[6] In the case of larger biological samples, RF power absorption in tissues requires a lower operating frequency. X-Band (9–10 GHz) EPR spectroscopy is therefore used for samples volumes of a few microlitres, L-band (1–2 GHz) for samples of few cm^3, and very low frequencies (200–300 MHz) are used for larger samples up to 200 cm^3.

Most *in vivo* experiments are currently performed at L-band on mice or isolated organs. L-Band spectrometers have also been used to obtain EPR images of geometrical phantoms,[7] plants[8] and implanted murine tumours.[9] In L-band experiments two kinds of resonator are currently used: surface coils and lumped parameter resonators. The former are helices or flat single-turn loops.[10] The depth sensitivity is limited due to the exponential decay of the microwave power inside the sample. Resonant cavities (reentrant and loop-gap), on the contrary, are designed to enclose the sample and are sensitive to the whole volume.[11,12] They make it possible to minimize the electric field inside the sample and can be designed to operate at very low frequencies. Loop-gap resonators have recently been used to obtain two-dimensional (2-D) images of mouse lung at 1.2 GHz,[13] three-dimensional (3-D) images of a rat head at 700 MHz,[14] and 2-D images of rat whole body at 280 MHz.[15] These results are summarized in Tables 2–4.

The use of small resonant cavities or surface detectors, which are volume selective, can help to distinguish the contribution of single organs to total nitroxide reduction. However, a proper volume picture of nitroxide distribution requires a complete 3-D image acquisition. The recording time in this case is currently longer than the half-life of available low toxicity nitroxides.

Table 1 Paramagnetic probes utilized in *in vivo* EPR spectroscopy/imaging

Spin probe	Feature
Aminoxyls	
Deuteriated/perdeuteriated aminoxyls	Narrow line
Fusinite	O_2 sensitive[1]
Lithium phthalocyanine (LiPc)	O_2 sensitive[1]
Carbohydrate char	O_2 sensitive[2]
Dextran magnetite	NMR contrast agent[3]
3-Propanenolic pyrrolin nitroxide	Specific for liver enzymes[4]
Doxyl stearate in lipid mixture	Temperature probe[5]

Table 2 Examples of EPR imaging at X-band

Sample size	Resolution	Spin probe	Sample	Image
1 mm	40 μm	Labelled stearic acid	Phospholipid vesicles + myelin	1-D Images by modulated gradients[16]
5 mm	50 μm	^{15}N-PDT	Excised fat and muscle	O_2 Sensitive[17] 2-D images 20 projections 25–30 G/cm
5 mm	200 μm	^{15}N-PDT	Rat femur	3-D Images[18] spectral–spatial 19 projections 25 G/cm
0.8 mm	10–20 μm	^{15}N-PDT	Spheroids (tumour)	2-D Images[19] 64 Projections 90 G/cm
0.8 mm	25 μm	DTBA	Skin biopsies of mouse	2-D Images[20] Spectral-spatial 400 G/cm
20 mm	1000 μm	Peroxyl radical	Broiled coffee bean chestnut	Scanning EPR[21]

[15] N-PDT: [1-^{15}N,$^{2}H_{16}$]-2,2,6,6-tetramethyl-4-oxopiperidin-1-yloxyl; DTBA: Di-*tert*-butylaminoxyl.

Table 3 Examples of EPR spectroscopy/imaging at L-band

Cavity size	Resonant cavity	Sample	Spin probe	Experiment
25 mm	Loop-gap 1 GHz	Capsule in peritoneal cavity of mouse	^{15}N-PDT	O_2 Sensitive localized detection in different breathing conditions[22]
5 mm	Surface coil 1.1 GHz	Mouse liver bladder head	TEMPONE[b] CAT1 PCA	Localized kinetics[23]
12 mm	Reentrant cavity 1.2 GHz	Rat rail	CTpO[d]	Localized kinetics[24]
12 mm	Reentrant cavity 1.2 GHz	Rat tail	TEMPO[a]	3-D Image[25] sequential 2-D 32 projections
33 mm	Loop-gap 1.3 GHz	Dead mouse lung; liver bladder blood	TEMPOL[e] C-PROXYL[f]	2-D Image 18 projections localized kinetics[13,26]
33 mm	Loop-gap 1.3 GHz	Mouse head abdomen	TEMPOL[e] C-PROXYL[f]	Localized kinetics in hypo/hyperoxia[27]
13 mm	Loop-gap 1.1 GHz	Perfused rat heart	TEMPO[a]	Clearance hypoxia[28,29]
15 mm	Reentrant cavity 1.5 GHz	Perfused rat heart	TEMPO[a] CTPO[g]	Clearance[30]
5 mm	Surface coil 1.1 GHz	Rat heart	Fusinite LiPc	Hypoxia, localization[1]

[a] TEMPO: 2,2,6,6-tetramethylpiperidin-1-yloxyl. [b] TEMPONE: 4-oxo-TEMPO. [c] CAT1: 2,2,6,6-tetramethyl-4-trimethylammoniopiperidin-1-yloxyl. [d] CTpO: 3-carbamido-2,2,5,5-tetramethylpyrrolidin-1-yloxyl. [e] TEMPOL: 4-hydroxy-TEMPO. [f] C-PROXYL: 3-Carbamoyl-2,2,5,5-tetramethylpyrrolidin-1-yloxyl. [g] CTPO: 3-Carbamoyl-2,2,5,5-tetramethyl-3-pyrrolin-1-yloxyl.

Table 4 Examples of EPR spectroscopy/imaging at very low frequency

Cavity size	Resonant cavity	Sample	Spin probe	Experiment
5 cm	Loop-gap 280 MHz	Whole rat	PCA	Kinetics; 2-D Transversal image[15]
2.5 cm	Loop-gap Strip-line type 250 MHz	Whole mouse	CTPO Different specific nitroxide liver specific	2-D Longitudinal image spectral-spatial[4]
5 cm	Loop-gap 300 MHz	Phantoms	DPPH[a] ^{15}N-PDT	Spectra[3]
2.4 cm	Reentrant 680 MHz	Mouse head liver bladder	PCA	Localized kinetics hypoxia[32,33]
4.1 cm	Loop-gap 710 MHz	Rat head	CTPO TEMPOL C-PROXYL	Kinetics[14] 3-D image 10 G/cm

[a] DPPH: 2,2-diphenyl-1-picrylhydrazyl hydrate.

The results of *in vitro* studies performed on tissue homogenates and cells cannot easily be extrapolated to *in vivo* conditions. Isolated organs such as the perfused rat heart represent better models and have been used to study nitroxide reduction and clearance with L-band spectrometers.[28,30] Attempts have been made to use this experimental model for the study of free radical generation by spin trapping techniques during ischemia/reperfusion,[34] but the sensitivity of present technology is limited. Recently nitroxide reduction has also been investigated directly *in vivo* in circulating blood at X-band.[35]

The aim of the present paper is to show the potential of *in vivo* EPR spectroscopy at different frequencies and to discuss the different experimental procedures that have been used. A deeper understanding of the distribution and metabolism of nitroxides is provided by an analysis of the PCA pharmacokinetics at three different frequencies in a blood circuit, a mouse head and rat whole body. The examples demonstrate the possibility of obtaining images of a moving phantom that mimics the heart at L-band and of mapping the *in vivo* distribution of a nitroxide by low frequency EPRI.

Experimental

L-Band Experiments.—L-Band experiments were performed on a home made EPR spectrometer integrated with three perpendicular sets of air coils that generate the gradients required for image reconstruction.[7] The apparatus has a three arm reentrant cavity operating at 1.3 GHz with an insertion diameter of 12 mm. This apparatus was used to investigate the *in vivo* pharmacokinetics of different nitroxides in a rat tail and to obtain 3-D images of the distribution of a nitroxide free radical injected in the rat vascular system.[25]

The same apparatus has been adapted to study an isolated rat heart with a larger cavity (diameter 15 mm, frequency 1.5 GHz). Hearts were retrogradely perfused using the Langendorff technique, and paced at 250 pulse/min.[30] The perfusion apparatus has two circuits containing the perfusion solution with and without the nitroxide. This set-up made it possible

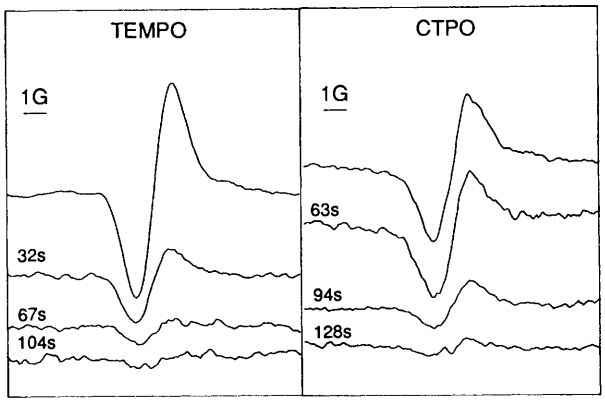

Fig. 1 L-Band spectra of the central line of two nitroxide species recorded in an isolated rat heart. The heart was perfused for about 20 min with Krebs solution containing 1 mmol dm^{-3} nitroxide. Spectra were collected at different times during the washout phase.

to reduce to a minimum the delay in the clearance of the paramagnetic probe due to the circuit. The control of a moving object in the resonant cavity is far from simple. The automatic frequency control (AFC) loop must be carefully adjusted to minimize the frequency noise caused by the heartbeat. This apparatus was used to determine the uptake and clearance of two nitroxides with different chemical properties: TEMPO (2,2,6,6-tetramethylpiperidinyloxyl) and CTPO (3-carbamoyl-2,2,5,5-tetramethyl-3-pyrrolin-1-yloxyl). The very fast clearance of these spin labels and the sampling rate of our apparatus did not allow for an accurate calculation of the kinetics parameters. Half-lives ranged between 70–90 s, much shorter than previously reported[28] (see Fig. 1). In these conditions the clearance rate depended on the perfusion rate as well as on the cell permeability to different nitroxides.

The possibility to map nitroxides in selective areas of the heart is extremely attractive. To this end a dynamic imaging system was designed that could be applied to the beating heart, consisting of an electronic device able to synchronize the signal acquisition with a stimulus generated by the same instrument.[36] This technique was tested on moving phantoms of the size of a rat heart. The phantom consisted of a latex balloon (volume 1.3 cm^3, dimensions 12 × 17 mm), inflated and deflated by a peristaltic pump. The variation in phantom volume inside the cavity disturbed the cavity coupling and reduced the S/N. To overcome this problem, the balloon was plunged into a tube filled with deionized water which was inserted in the cavity. Synchronized acquisition made it possible to collect 16 spectra at fixed fractions of the period during each field scan. A 2-D image acquisition thus generates 16 images at different positions during the movement cycle of the phantom. Fig. 2 presents 6 images of the dynamic phantom, in which differences can be observed in the lower part of the balloon. The shape can be explained by the fact that the actual compression of the balloon was completely asymmetrical and a concavity was produced in the balloon wall.

680 MHz *and* 280 MHz *Experiments.*—Experiments on whole mice were performed at 680 MHz with a Hewlett Packard 8640B signal generator as RF source and a reentrant three arm cavity with an insertion diameter of 24 mm and an active region length of 3 cm. By shifting the mouse in relation to the active region of the resonator[33] it was possible to obtain spectra from different parts of the mouse. The spin label used was PCA (3-carboxy-2,2,5,5-tetramethylpyrrolidin-1-yloxyl) which was chosen for its low toxicity and slow rate of reduction, which depends on oxygen concentration.[37] PCA clearance was investigated with the aim of detecting possible variations in clearance time due to changes in animal oxygenation.[32] The maximum sample size observed at this frequency was about 20–25 g. The size of these animals made artificial ventilation impossible. Therefore, bigger animals on which respiratory control can be applied are necessary for more appropriate physiological studies.

A typical PCA clearance observed in a mouse head region is shown in Fig. 3. This clearance is compared with two clearances obtained on a rat whole body with a 280 MHz apparatus and on rat circulating blood with an X-band apparatus.

A 280 MHz apparatus based on a cylindrical 16 pole magnet was developed and designed specifically for the imaging of 50–200 g laboratory animals. It generated the main field up to 0.02 T and two of the three field gradients required for 3-D imaging. The third gradient was provided by air coils inside the magnet. Field and gradient direction could be rotated under computer control, making image reconstruction very similar to that used in computer assisted tomography.[38] The RF section consisted of a reflection cavity homodyne bridge and a loop-gap resonator 4.9 cm in diameter and 10 cm in length with an operating frequency of about 280 MHz.

This apparatus has made it possible to study PCA pharmacokinetics as well as to obtain 2-D images of the whole body of temperature- and blood pressure-controlled rats.[15] A typical PCA clearance curve from rat whole body is reported in Fig. 3. The rat head was placed outside the resonator and because of the non-uniform RF distribution inside the loop-gap cavity, the extremities (upper abdomen and bladder region) of the rat gave a reduced contribution to the total signal. Fig. 4 shows a typical 2-D transversal image after PCA injection. The acquisition of 8 projections took about 6 minutes and two sets of projections could be collected during one kinetic run.[15] The 2-D images obtained by EPRI represent the projections on a plane of the whole volume distribution of the paramagnetic probe. For this reason it was almost impossible to associate the observed distribution of spin density with particular organs. A more meaningful map of the nitroxide distribution could be obtained from 2-D longitudinal images, which can distinguish the various organs along the spinal axis of a rat.[39]

In order to evaluate the contribution of blood to the whole body clearance, PCA pharmacokinetics were also studied directly in rat circulating blood (Fig. 3). To this end a thin silastic tube was inserted between the carotid arteries and positioned in the X-band cavity. The clearance in circulating blood showed a fast distribution phase followed by a slow reduction/elimination phase. The distribution phase coincided with the transfer of nitroxide from blood to tissue compartment. Conversely, the clearances performed on intact animals at lower frequencies could not detect this phase and presented a monoexponential decay.

Small differences between the half-lives found in the three experimental models may be due to many factors: the different animal species involved, different organs monitored, animal sizes, animal temperatures, PCA doses, or animal stress due to surgical procedures, *etc.* However, since blood performs no reductive activity,[40] the clearance measured in the blood reflects the total effect of all tissues and is very similar to whole body clearance.

Discussion

In the search for an optimal experimental apparatus, the RF losses in living samples pose problems of frequency, geometrical structure and the dimensions of the resonator. These problems are very different from those present in X-band spectroscopy. In the range of conductivity of biological samples, RF losses are due to both the electrical and magnetic RF fields. It has been shown[41] that multi-gap structures can significantly reduce

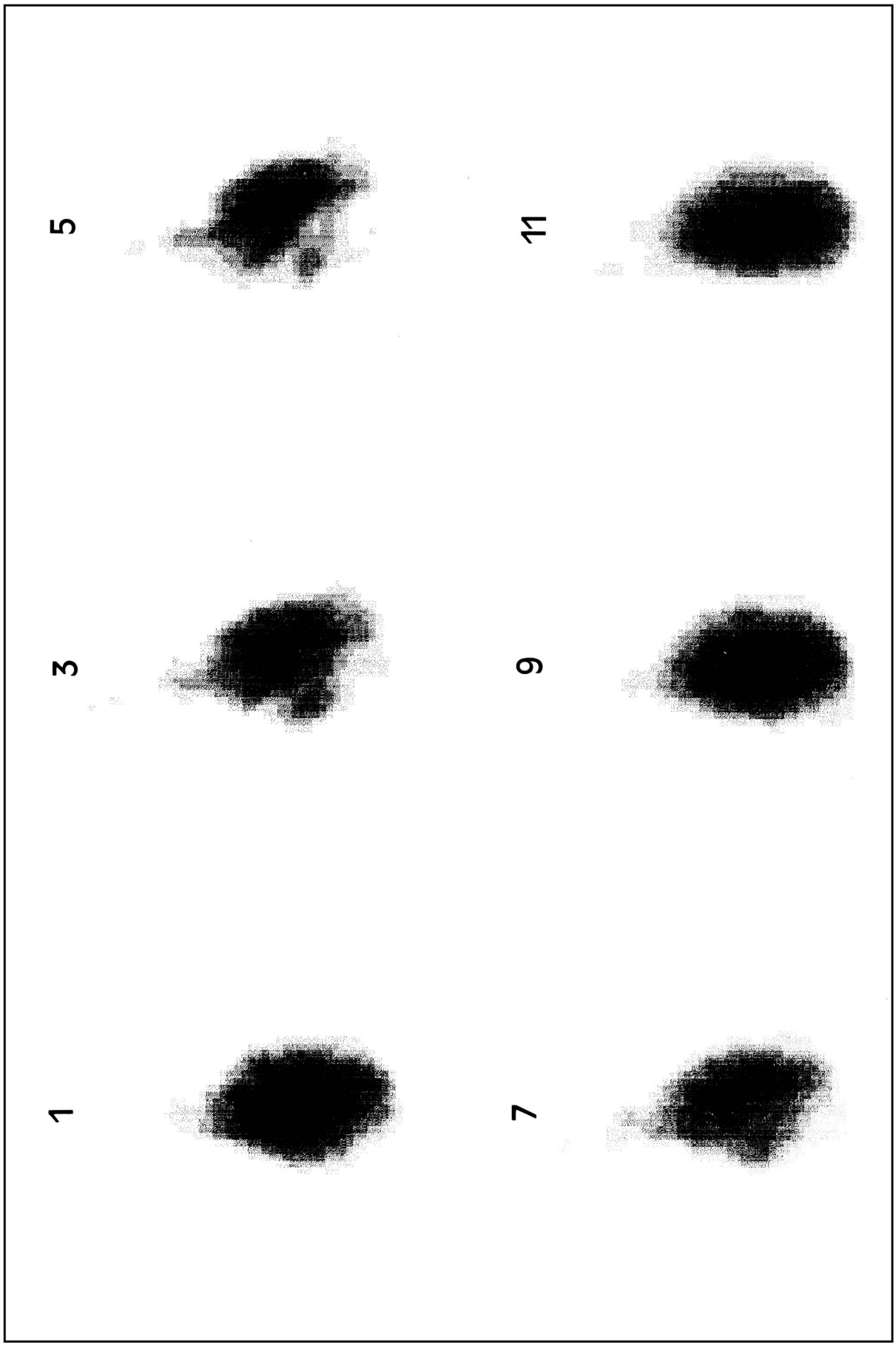

Fig. 2 2-D images collected during the movement cycle of the phantom described in the text. Images were collected at 1,3,5,7,9,11 sixteenths of a 1.5 s period. The phantom contained 1 mmol dm^{-3} Fremy's salt. Acquisition time: 40 min for 16 projections. Gradient value 43 mT/m. Images are 64 × 64 pixels scaled in eight grey levels. The signals lower than 12.5% of the maximum were regarded as noise.

electric field loss so that the dominant effect is due to the magnetic field loss. The equivalent circuit of a conductive cylindrical sample is a dissipative resistance whose value is directly proportional to the square of the frequency and to the fourth power of the radius.[42] This dissipative element lowers the resonator Q (quality factor), lowering the S/N. Once the sample volume and geometrical shape are fixed, the only way to optimize the S/N is by a proper selection of the operating frequency and by optimizing the resonator diameter in relation to the size of the sample.[42]

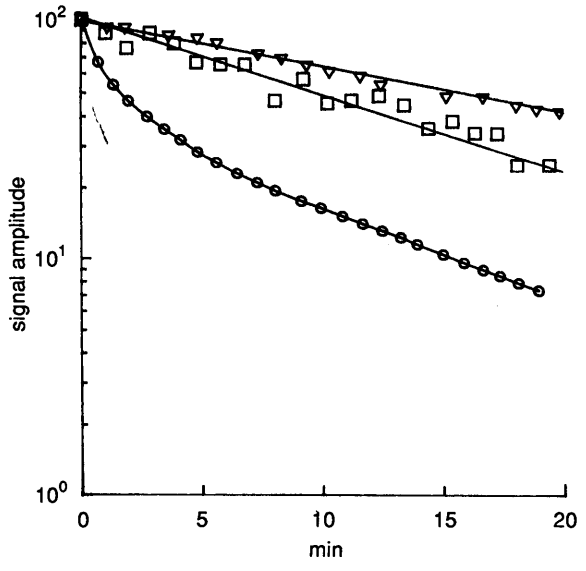

Fig. 3 Three PCA clearances in different *in vivo* models after 0.44 mmol kg^{-1} intravenous injection. The experimental conditions were as follows: (1) 680 MHz reentrant cavity including the whole body of a 20 g mouse with active region centred on the mouse head, ▽; (2) 280 MHz loop-gap cavity 10 cm in length and 4.9 cm in diameter which contained a rat whole body, □; (3) external blood circulation shunt on a 150 g rat observed at X-band, 9500 MHz ○. Signal amplitude was the peak to peak height of the central component of the PCA triplet. Spectra collected at 680 MHz were filtered to cut the oscillating pattern originated by the rhythmical respiratory movements in the head region. Half lives for the mouse head and whole rat were 15.1 and 10.5 min respectively. Half life of the slow phase measured in the circulating blood was 7.7 min.

As an example, the minimum detectable molar concentration observed at 280 MHz with a cylindrical sample holder 2.8 cm in diameter and containing 50 cm^3 of Fremy's salt (potassium nitrosodisulfonate) solution, 0.05 mT in line width, was 4 μmol dm^{-3}. At L-band, with the sample used to simulate heart movements filled with PCA, 0.16 mT in line width, we observed a minimum detectable concentration of 5 μmol dm^{-3}. However, no attempts were made to work with the same filling factor, so that this comparison is only approximate. It is important, however, that in this frequency range experimental evidence shows only a small decline in the S/N with frequency and that for samples with line widths of about 0.1 mT a minimum detectable concentration between 1 and 10 μmol dm^{-3} can still be observed. The sweepable RF source used for the 280 MHz apparatus has a frequency modulation noise much higher than quartz stabilized sources. Single frequency spectrometers[31] have been shown to have a better minimum detectable molar sensitivity, in the range of 0.1 μmol dm^{-3}.

At the present stage of development, EPRI makes it possible to approach a large variety of biological problems related to the distribution and metabolization of paramagnetic probes. The technique is still far from being a satisfactory imaging tool for the following reasons. First, the EPR image is known to be particularly sensitive to the non-homogeneity of the magnetic field and to the non-linearity of the field gradients and these aspects still call for considerable research. Moreover, all the resonators currently used have a non-homogeneous RF field distribution, particularly along the axial direction.[14,43,44] This affects image reconstruction, in fact signal intensity is proportional to the RF field intensity, for continuous wave apparatus

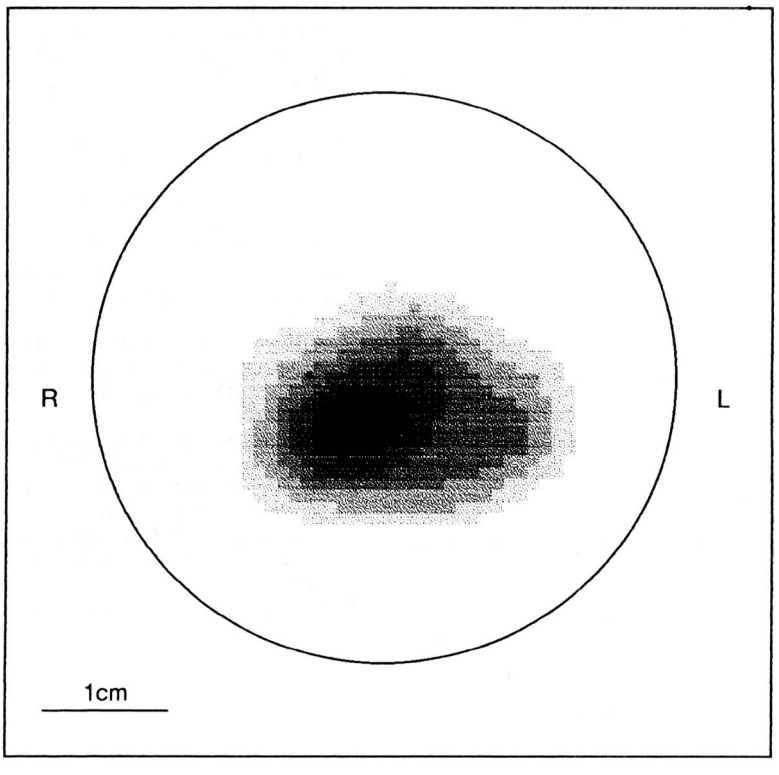

Fig. 4 Transversal two-dimensional image of PCA distribution in the body of a 54 g rat. Acquisition started 3 min after the intravenous injection (1 mmol kg^{-1}) of PCA. The circle shows the area inside the cavity. The image was reconstructed from 8 projections collected with 25 mT/m gradient at 280 MHz for a total acquisition time of 6 min and was reproduced in six grey levels.

far from saturation. To avoid this problem, larger resonators should be used, but this would reduce the sample filling factor and, therefore, sensitivity. The second major problem is the line width of the paramagnetic probes currently used. Most research is now being done with commercial nitroxide free radicals with a line width of the order of 0.14–0.16 mT.[45] This greatly affects the resolution, especially in the presence of a low S/N. The use of probes with large line widths could be overcome by using a larger field gradient, but this distributes the resonance line over a larger field region, reducing the S/N. This acquires increasing importance when considering large samples. In our experience with biological samples of about 5 cm it is difficult to use field gradients larger than 0.015–0.020 T/m. Gradients of this size distribute the resonance in a region of about 1 mT, reducing the signal at the level of the noise. The third major problem is the data acquisition time necessary for image reconstruction. It takes about 4–6 min for a 2-D and much longer for a 3-D reconstruction, thereby making the *in vivo* use of this technique extremely problematical. In these conditions it is very difficult to explain the EPRI data on an anatomical basis, since the images reflect different factors, such as nitroxide distribution, metabolic activity, renal clearance.

A significant improvement would be the adoption of a pulsed EPR technique. With an identical S/N this should greatly reduce the acquisition time, permitting the acquisition of projections for 2-D and 3-D image reconstruction in times compatible with biological processes. The relaxation times of most organic radicals (around 100 ns) don't allow for the fast gradient pulsing used in NMR spectroscopy for field-gradient encoded imaging, but other pulsed experiments are possible with stationary field gradients. The other major improvement that should emerge from cooperation with chemists is the development of biological compatible, narrow bandwidth, single line paramagnetic probes.

The results presented in this paper show examples of the potential and limitations of today's EPRI technology. In spite of the discussed limitations, EPRI makes possible a variety of biological applications. New prospects could be opened up by the development of very narrow line width and/or selective probes and by the adoption of pulsed techniques.

Acknowledgements

This work was supported in part by MURST 40%, INFN, INFM and P.F. CNR ACRO.

References

1 J. F. Glockner and H. M. Swartz, *Adv. Exp. Med. Biol.*, 1992, **317**, 229.
2 S. W. Norby, A. I. Smirnow, S. Boyer, H. M. Swartz and R. B. Clarkson, *11th Annual Scientific Meeting Soc. Magn. Reson. in Med.*, 1992, abs. 4107.
3 A. Iannone, R. L. Magin, T. Walczak, M. Federico, H. M. Swartz, A. Tomasi and V. Vannini, *Magn. Reson. Med.*, 1991, **22**, 435.
4 H. J. Halpern, C. Yu, E. Barth, M. Peric, W. E. Boisvert, M. V. Makinen, S. Pou and G. M. Rosen, *34th Rocky Mountain Conference on Analytical Chemistry*, 1992, abs. 177.
5 H. M. Swartz, K. Liu, G. C. Chato, M. V. Grinstaff and K. S. Suslick, *34th Rocky Mountain Conference on Analytical Chemistry*, 1992, abs. 178.
6 J. H. Freed, *J. Chem. Soc., Faraday Trans.*, 1990, **86**, 3173.
7 S. Colacicchi, P. L. Indovina, F. Momo and A. Sotgiu, *J. Phys. E: Sci. Instrum.*, 1988, **21**, 910.
8 H. Fujii and L. J. Berliner, *Magn. Reson. Med.*, 1985, **2**, 275.
9 L. J. Berliner, H. Fujii, X. Wan and S. J. Lukiewicz, *Magn. Reson. Med.*, 1987, **4**, 380.
10 H. Nishikawa, H. Fujii and L. J. Berliner, *J. Magn. Reson.*, 1985, **62**, 79.
11 A. Sotgiu, *J. Magn. Reson.*, 1985, **65**, 206.
12 W. Froncisz and J. S. Hyde, *J. Magn. Reson.*, 1982, **47**, 515.
13 K. Takeshita, H. Utsumi and A. Hamada, *Biochem. Biophys. Res. Commun.*, 1991, **177**, 874.
14 S. Ishida, S. Matsumoto, H. Yokoyama, N. Mori, H. Kumashiro, N. Tsuchihashi, T. Ogata, M. Yamada, M. Ono, T. Kitajima, H. Kamada and E. Yoshida, *Magn. Reson. Imag.*, 1992, **10**, 109.
15 V. Quaresima, M. Alecci, M. Ferrari and A. Sotgiu, *Biochem. Biophys. Res. Commun.*, 1992, **183**, 829.
16 T. Pali, B. Ebert and L. I. Horvath, *Biochim. Biophys. Acta*, 1987, **904**, 346.
17 G. Bacic, T. Walczak, F. Demsar and H. M. Swartz, *Magn. Reson. Med.*, 1988, **8**, 209.
18 R. K. Wood, G. Bacic, P. C. Lauterbur and H. M. Swartz, *J. Magn. Reson.*, 1989, **84**, 247.
19 J. W. Dobrucki, F. Demsar, T. Walczak, R. K. Woods, G. Bacic and H. M. Swartz, *Br. J. Cancer*, 1990, **61**, 221.
20 J. Fuchs, H. J. Freisleben, N. Groth, T. Herrling, G. Zimmer, R. Milbradt and L. Packer, *Free Radical Res. Commun.*, 1991, **15**, 245.
21 M. Ikeya, *Magnetic Resonance Microscopy*, Verlagsgesellschaft, Weinheim, 1992.
22 W. K. Subczynski, S. Lukiewicz and J. S. Hyde, *Magn. Reson. Med.*, 1986, **3**, 747.
23 G. Bacic, M. J. Nilges, R. L. Magin, T. Walczak and H. M. Swartz, *Magn. Reson. Med.*, 1989, **10**, 266.
24 L. J. Berliner and X. Wan, *Magn. Reson. Med.*, 1989, **9**, 430.
25 M. Alecci, S. Colacicchi, P. L. Indovina, F. Momo, P. Pavone and A. Sotgiu, *Magn. Reson. Imag.*, 1990, **8**, 59.
26 H. Utsumi, E. Muto, S. Masuda and A. Hamada, *Biochem. Biophys. Res. Commun.*, 1990, **172**, 1342.
27 Y. Miura, H. Utsumi and A. Hamada, *Biochem. Biophys. Res. Commun.*, 1992, **182**, 1108.
28 J. L. Zweier and P. Kuppusamy, *Proc. Natl. Acad. Sci. USA*, 1988, **85**, 5703.
29 J. L. Zweier, S. T. Gorman and P. Kuppusami, *J. Bioenerg. Biomembr.*, 1991, **23**, 855.
30 P. Gallo, S. Colacicchi, M. Ferrari, G. Gualtieri and A. Sotgiu, *Cardioscience*, 1991, **2**, 221.
31 J. A. Brivati, A. D. Stevens and M. C. R. Symons, *J. Magn. Reson.*, 1991, **92**, 480.
32 S. Colacicchi, M. Ferrari, G. Gualtieri, M. T. Santini and A. Sotgiu, *Phys. Med.*, 1989, **5**, 297.
33 M. Ferrari, S. Colacicchi, G. Gualtieri, M. T. Santini and A. Sotgiu, *Biochem. Biophys. Res. Commun.*, 1990, **166**, 168.
34 J. L. Zweier, P. Kuppusamy, R. Williams, B. K. Rayburn, D. Smith, M. L. Weisfeldt and J. T. Flaherty, *J. Biol. Chem.*, 1989, **264**, 18890.
35 X. Wang, J. Liu, I. Yokoi, M. Kohno and A. Mori, *Free Radical Biol. Med.*, 1992, **12**, 121.
36 L. Testa, G. Gualtieri and A. Sotgiu, *Phys. Med. Biol.*, 1992, **37**, 1.
37 K. Chen, J. F. Glockner, P. D. Morse II and H. M. Swartz, *Biochemistry*, 1989, **28**, 2496.
38 M. Alecci, S. Della Penna, A. Sotgiu and L. Testa, *Appl. Magn. Reson.*, 1992, **3**, 909.
39 M. Alecci, M. Ferrari, R. Passariello, V. Quaresima, A. Sotgiu and C. L. Ursini, *XI Annual Meeting Soc. Magn. Reson. in Med.*, 1992, abs. 4110.
40 W. R. Couet, U. G. Eriksson, T. N. Tozer, L. D. Tuck, G. E. Wesbey, D. Nitecki and R. C. Brasch, *Pharm. Res.*, 1984, 203.
41 M. Alecci, G. Gualtieri and A. Sotgiu, *J. Phys. E: Sci. Instrum.*, 1989, **22**, 354.
42 P. Mansfield and P. G. Morris, *NMR Imaging in Biomedicine*, Academic Press, Orlando, 1982.
43 M. Alecci, S. Della Penna, A. Sotgiu, L. Testa and I. Vanucci, *Rev. Sci. Instrum.*, 1992, **63**, 4263.
44 H. J. Halpern, D. P. Spencer, J. van Polen, M. K. Bowman, A. C. Nelson, E. M. Dowey and A. B. Teicher, *Rev. Sci. Instrum.*, 1989, **60**, 1040.
45 S. Colacicchi, M. Ferrari and A. Sotgiu, *Int. J. Biochem.*, 1991, **24**, 205.

Paper 3/01943H
Received 30*th March* 1993
Accepted 4*th May* 1993